THE JOURNAL OF BIOLOGICAL CHEMISTRY VOL. 289, NO. 37, pp. 25556–25570, September 12, 2014

Ligands for FKBP12 Increase Ca^{2+} Influx and Protein Synthesis to Improve Skeletal Muscle Function*

Received for publication, June 11, 2014, and in revised form, July 9, 2014 Published, JBC Papers in Press, July 22, 2014, DOI 10.1074/jbc.M114.586289

Chang Seok Lee[‡1], Dimitra K. Georgiou[‡1], Adan Dagnino-Acosta[‡1], Jianjun Xu[‡2], Iskander I. Ismailov[‡3], Mark Knoblauch[‡], Tanner O. Monroe[‡], RuiRui Ji[‡], Amy D. Hanna[‡], Aditya D. Joshi[‡], Cheng Long[‡4], Joshua Oakes[‡], Ted Tran[‡], Benjamin T. Corona[§], Sabina Lorca[¶], Christopher P. Ingalls[§], Vihang A. Narkar[¶], Johanna T. Lanner[‡5], J. Henri Bayle[‡], William J. Durham[‖], and Susan L. Hamilton[‡6]

From the [‡]Baylor College of Medicine, Houston, Texas 77030, the [§]Muscle Biology Laboratory, Department of Kinesiology and Health, Georgia State University, Atlanta, Georgia 30302, the [¶]Center for Metabolic and Degenerative Disease, University of Texas Health Science Center, Houston, Texas 77030, and the [‖]Department of Internal Medicine, University of Texas Medical Branch, Galveston, Texas 77555-1041

Background: Rapamycin is a known inhibitor of protein synthesis but also modulates the activity of RyR1.
Results: FKBP12 deficiency and low doses of either rapamycin or SLF increase, rather than decrease, protein synthesis and improve muscle function.
Conclusion: In skeletal muscle, FKBP12 regulates Ca^{2+} influx, Ca^{2+} store refilling, and protein synthesis.
Significance: This study lays the groundwork for the development of interventions to slow muscle fatigue.

Rapamycin at high doses (2–10 mg/kg body weight) inhibits mammalian target of rapamycin complex 1 (mTORC1) and protein synthesis in mice. In contrast, low doses of rapamycin (10 μg/kg) increase mTORC1 activity and protein synthesis in skeletal muscle. Similar changes are found with SLF (synthetic ligand for FKBP12, which does not inhibit mTORC1) and in mice with a skeletal muscle-specific FKBP12 deficiency. These interventions also increase Ca^{2+} influx to enhance refilling of sarcoplasmic reticulum Ca^{2+} stores, slow muscle fatigue, and increase running endurance without negatively impacting cardiac function. FKBP12 deficiency or longer treatments with low dose rapamycin or SLF increase the percentage of type I fibers, further adding to fatigue resistance. We demonstrate that FKBP12 and its ligands impact multiple aspects of muscle function.

The macrolide rapamycin is a potent and widely used immunosuppressant that, at doses from 2 to 10 mg/kg has many beneficial physiological effects in mice (1), including increased life span (2); improved cognitive function (3); and alleviation of symptoms of cancer (4, 5), tuberous sclerosis complex (6), Alzheimer disease (3), Leigh syndrome (7), and muscle disease (8). Most of these effects are ascribed to the inhibition of mammalian target of rapamycin complex 1 (mTORC1)[7] (9, 10). To effect this mechanism, rapamycin acts as a pro-drug that binds to FKBP12 (FK506-binding protein 12 kDa) creating a composite surface that binds to the protein kinase mTOR, blocking phosphorylation of mTORC1 targets. This decreases protein synthesis and promotes autophagy. However, FKBP12 is a peptidylprolyl isomerase and a binding partner for several important signaling proteins (11–13). FKBP12 ligands, including rapamycin, FK-506, ascomycin, and the synthetic molecule SLF (synthetic ligand for FKBP12), can disrupt these interactions (14, 15).

FKBP12 binding to the skeletal muscle Ca^{2+} release channel RyR1 stabilizes a closed state of the channel to minimize Ca^{2+} leak from the sarcoplasmic reticulum (SR) (11). FKBP12 also binds to TGFβR1 and slows phosphorylation by TGFβR2 to decrease TGFβ signaling at low ligand concentrations (12) and binds to palmitoylated Ras to promote depalmitoylation and movement from the plasma membrane to the endoplasmic reticulum/Golgi (13). At present, there is little information regarding alternative protein targets of FKBP12 and their role in the physiological effects of rapamycin in skeletal muscle.

* This work was supported, in whole or in part, by National Institutes of Health Grants AR41802 and AR053349 (to S. L. H.). This work was also supported in part by grants from the Muscular Dystrophy Association and the United States Department of Defense.
[1] These authors contributed equally to this work.
[2] Present address: Graduate school of Medicine and Dental Science, Kagoshima University, Sakura-ga-oka, 890-8520 Kagoshima.
[3] Present address: Virginia Tech Carilion Research Institute, Virginia Polytechnic Institute and State University, 2 Riverside Circle, VT Mail Code 0801, Roanoke, VA 24016. Tel.: 540-526-2054.
[4] Present address: School of Life Sciences, South China Normal University, Guangzhou 510631, China.
[5] Supported by a postdoc fellowship from The Swedish Research Council. Present address: Karolinska Institutet, Dept. of Physiology and Pharmacology, von Eulersvag 8, 171 77 Stockholm, Sweden.
[6] To whom correspondence should be addressed: Dept. of Molecular Physiology and Biophysics, Baylor College of Medicine, 1 Baylor Plaza, Houston, TX 77030. Tel.: 713-798-3894; Fax: 713-798-5441; E-mail: susanh@bcm.tmc.edu.

[7] The abbreviations used are: mTORC1, mammalian target of rapamycin complex 1; mTOR, mammalian target of rapamycin; FKBP12D, mouse heterozygous for floxed FKBP12 gene and heterozygous for FKBP12 knockout (lox/null) expressing CRE recombinase under the muscle creatine kinase promoter; RyR1, sarcoplasmic reticulum Ca^{2+} release channel in skeletal muscle or ryanodine receptor; RyR3KO, mice with a general knockout of RYR3 generated by H. Takeshima; SR, sarcoplasmic reticulum; $Ca_V1.1$, skeletal L-type voltage-dependent calcium channel; FDB, flexor digitorum brevis; EDL, extensor digitorum longus; SERCA, SR Ca^{2+}-ATPase; CSQ, calsequestrin; ERR, estrogen-related receptor; PPAR, peroxisome proliferator-activated receptor; SLF, synthetic ligand for FKBP12; BTS, 4-methyl-*N*-(phenylmethyl)benzenesulfonamide.

Excitation-contraction coupling in skeletal muscle culminates in the release of Ca^{2+} from the SR to the cytoplasm, leading to force development. For the muscle to contract, the depolarization of the transverse tubule membrane in response to a signal from the nerve induces a conformational change in the voltage-dependent Ca^{2+} channel, $Ca_V1.1$, which, in turn, mechanically gates the opening of RyR1, releasing Ca^{2+} from SR Ca^{2+} stores. Muscle relaxation requires a decrease in the cytoplasmic Ca^{2+} levels, the majority of which is pumped back into the store via SR Ca^{2+}-ATPase (SERCA).

With repetitive activation, skeletal muscle exhibits a decline in force generation, a process designated as fatigue. The rate at which muscle fatigues is inversely related to the proportion of oxidative, slow twitch, type I fibers, which fatigue more slowly than type II fibers (16). Skeletal muscle fiber type composition displays some plasticity and can be modulated by exercise (17), due to the activation of the calcineurin/NFAT (18) and estrogen-related receptor γ (ERRγ)/PPARβ/γ pathways (19). Interventions that activate these pathways also increase the proportion of type I fibers and slow muscle fatigue (20). The maintenance of SR Ca^{2+} stores and the magnitude of the Ca^{2+} transients are also critical factors in slowing muscle fatigue (18–21). *In vitro* repetitive contractions reduce SR Ca^{2+} stores and the amount of SR Ca^{2+} that is released, leading to skeletal muscle fatigue (21).

Given the multisystemic effects of rapamycin and FKBP12 modulation, it is important to determine whether alterations in FKBP12 and rapamycin targets other than mTORC1 contribute to the effects of this drug. In this paper, we explore the effects of genetic and pharmacological disruption of FKBP12 on Ca^{2+} signaling, protein synthesis, and function of skeletal muscle. We have evaluated the effects of low dose (10 μg/kg body weight) rapamycin and SLF (1 μg/kg body weight) on skeletal muscle function and compare the drug effects with a skeletal muscle-specific deficiency in FKBP12. SLF does not alter mTORC1 or calcineurin activity (22). We demonstrate that rapamycin, SLF, and muscle-specific deficiency in FKBP12 enhance the refilling of SR Ca^{2+} stores, turn on the slow fiber-type program, slow muscle fatigue, and improve running endurance in mice. We also show that these treatments increase, rather than decrease, protein synthesis. In our studies, the first detectable effect of both rapamycin and SLF is an alteration in Ca^{2+} influx to enhance refilling of Ca^{2+} stores. We propose that this is the primary mechanism whereby low doses of these drugs improve endurance. However, other targets may be involved in some of the other effects of low dose rapamycin and SLF.

MATERIALS AND METHODS

Drugs—Rapamycin was purchased from LC Laboratories, and SLF was purchased from Cayman Chemical Company.

Antibodies—Antibodies for phospho-S6 (Ser-235/236), S6, phospho-4-EBP1 (Thr-37/46), 4EBP1, phospho-Akt (Ser-473), phospho-Akt (Thr-308), Atg5, beclin 1, phospho-SMAD2 (Ser-465/467), SMAD2, phospho-eEF2 (Thr-56), and eEF2 were obtained from Cell Signaling. Antibodies for SERCA1, SERCA2, calsequestrin, RyR1, FKBP12, and $Ca_V1.1$ were obtained from Thermo Scientific. Antibodies for myoglobin, Akt, phospho-ERK (Thr-202/Tyr-204), and ERRα were obtained from Santa Cruz Biotechnology, Inc. Antibodies to MHC1 and MHC2a were from DSHB. The antibody to puromycin was obtained from Kerafast.

Mouse Models—The FKBP12D mice (skeletal muscle-specific FKBP12-deficient mice) were created in our laboratory as described by Tang *et al.* (23). Mice (CRE^+) expressing CRE^+ recombinase under the creatine kinase promoter were used as controls. The RyR3 knock-out mice were generously provided by Dr. H. Takeshima. Mice used were between 6 and 12 weeks of age except where indicated and were age-matched in each experiment. All mice were housed at room temperature with a 12-h/12-h light/dark cycle. Food and water were provided *ab libitum*. All procedures were approved by the Animal Care Committee at Baylor College of Medicine.

Echocardiography—Echocardiography was performed using a VisualSonics VeVo 770 Imaging System (VisualSonics, Toronto, Canada) with a 30-MHz probe. Mice were initially anesthetized with 2% isoflurane mixed with 100% O_2 and placed on a heated pad, where all four limbs were taped down onto copper electrocardiogram plates. On the plate, anesthesia was maintained with 1% isoflurane through a nose cone. A rectal temperature probe was used to monitor body temperature.

MHC Fiber Typing—Soleus, EDL, diaphragm, and flexor digitorum brevis (FDB) muscles were dissected, embedded (Tissue-Tek), and frozen in the 2-methylbutane (Sigma) precooled in the liquid nitrogen. The frozen muscles were sectioned at 10-μm thickness using a cryostat microtome (SHANDON Cryotome E, Thermo Electron Corp.). Sections were stained with myosin heavy chain-specific antibodies and isotype-specific secondary antibodies and imaged under the fluorescence microscope (Olympus). The relative numbers of the different fiber types were quantified and normalized by the total number of muscle fibers per field of images.

Calcineurin Activity Assay—Calcineurin activity was evaluated with a colorimetric assay kit from Calbiochem/Millipore. Diaphragm, soleus, and EDL muscle were homogenized according to the kit instructions and were desalted before the assay. Samples were incubated at 37 °C for 30 min. The activity was normalized to total protein in the sample homogenates.

SR Membrane and Homogenate Preparation—Homogenates from diaphragm, EDL, and soleus muscles were prepared in buffer containing 250 mM sucrose, 100 mM KCl, 5 mM EDTA, and 10 mM Tris-HCl, pH 6.8, and protease inhibitors as in the membrane preparations. Muscles were homogenized in the Precellys 24 tissue homogenizer and centrifuged in an Eppendorf microcentrifuge at 25,000 $\times$ *g* for 15 min. Supernatants were aliquoted, snap-frozen in liquid nitrogen, and stored at −80 °C until use. Protein concentration was measured by a Lowry and/or BCA assay.

Calculation of Percentage Occupancy of FKBP12 Sites on RyR1—Intracellular FKBP12 concentration was calculated using μmol of FKBP12/mg of protein in an aliquot of the homogenate, the amount of total protein, and volume of the muscle bundles. The volume was estimated from the mass and the density of 1.06 mg/ml. To approximate the "free concentration" of FKBP12, homogenates were separated into supernatants and pellets by centrifugation in a Beckman Airfuge under conditions where membranes, nuclei, and mitochondria are found in

the pellet and soluble proteins are found in the supernatant. To control for homogenization efficiency, we assessed the distribution of myoglobin in the supernatants and pellets using an anti-myoglobin antibody. The total amount of FKBP12 in each supernatant and pellet was calculated and corrected for the solubilization efficiency. To estimate the concentration of FKBP12 binding sites associated with RyR1, we multiplied the number of [^{3}H]ryanodine binding sites by 4 (one binding site per subunit of the homotetramer). The total RyR1 in muscle homogenates of the soleus, EDL, and diaphragm muscle in FKBP12D and CRE$^+$ mice using RyR (nM) was estimated from the expression, 1000 dBP/m, where d is the density of 1.06 mg/ml, B is the amount of RyR1 in the muscle estimated from [^{3}H]ryanodine binding in nmol/mg, P is the total protein measured in homogenates, and m is the mass of the muscle. We also determined the affinity of [^{35}S]FKBP12 for muscle membranes at room temperature ($K_D = 8.6 \pm 1.2$ nM, $n = 7$) and at 37 °C ($K_D = 27 \pm 2.2$ nM, $n = 3$). The estimated number of FKBP12s bound per RyR1 was determined in the soleus, EDL, and diaphragms of CRE$^+$ and FKBP12D mice. We estimate that in CRE$^+$ muscle, there is adequate FKBP12 to saturate >95% of the RyR1 binding sites, and despite a 80–90% decrease in tissue FKBP12 in the FKBP12D muscle, the saturation of RyR1 would decrease by <50% in most muscles.

Endurance Running—Endurance running was performed as described by Narkar *et al.* (20) with modifications.

Grip Strength—FKBP12D and CRE$^+$ mice (7.5–8.5 weeks old) were tested for grip performance on a grip strength meter from Columbus Instruments, according to the standard protocol from Jackson Laboratory. For each mouse, the test was repeated five consecutive times for both hind limb and forelimb together.

Fatigue—Fatigue studies were performed as described previously (24).

Manganese Quench Assay—Isolated FDB muscle fibers were loaded with 10 μM Fura-2/AM for 1 h at room temperature in DMEM in the presence of 20 μM BTS. The fluorescent signal of preloaded fibers was monitored with a calcium-insensitive excitation filter, 360 nm, placed in a Lambda DG4 system used as light source. Emitted florescence was collected through a Nikon S. Fluor objective (×20, 0.75 numerical aperture) coupled to an inverted microscope (Nikon eclipse TE-200) and digitized using a CCD Rolera MGi-Plus camera with 510 × 252 pixels field size (using 6 binning). Data were collected and stored in the computer using the Metafluor software (version 6.2) for further analysis. The fluorescent signal was measured during 5 min in the presence of normal Tyrode buffer, and then $CaCl_2$ was replaced with $MnCl_2$ (1.8 mM) for the rest of the experiment; at min 10, the focused FDB was stimulated with 20 trains. Electrical stimulation was performed using two platinum wires placed at each side of the fiber oriented longitudinally, and one electrical train (50 Hz, 1 s duration) was applied every 5 s (20 trains total).

Ca^{2+} Measurements—Note that myofibers were loaded with the Ca^{2+} indicators at room temperature because we found that 37 °C loading caused the dyes to partition into various organelles and gave results very different from those we are currently reporting. To monitor the Ca^{2+} release kinetics with electrical stimulation, FDB fibers were loaded with 5 μM Mag-Fluo4 for 30 min at room temperature in the presence of 20 μM BTS. Loaded FDBs were perfused with Tyrode buffer with 20 μM BTS at 0.5 ml/min) and imaged in line scan mode (one line was acquired every 1.15 ms (3.66 μs/pixel time) using a ×20 objective (EC Plan-Neofluar) mounted in the confocal microscope (Zeiss LSM 510 meta)). Dye was excited at 488 nm, and emitted light was collected through an LP 505-nm filter.

Western Blots—Western blots were performed as described previously (24). To control for variations among different Western blots and allow for multiple repeats, the absorbance intensity for each Western blotted band was normalized to the absorbance intensity of the corresponding band from the control mice (WT, CRE$^+$, or WT saline) from the same Western blot, averaged with values obtained from other Western blots, and plotted as a percentage of control. Some blots had multiple controls, and the absorbance of the specific band was normalized to the average.

Detection of Puromycin-labeled Proteins—Mice (6–8 weeks of age) were food-deprived for 6 h and refed for 2 h.

Propofol (18 μl/g) was injected (intraperitoneally) in mice after 70 min of refeeding. The mice were then injected (intraperitoneally) with puromycin (0.04 μmol/g body weight), and the mice were sacrificed 35 min later. Muscles were isolated, homogenized, and prepared for Western blotting with antipuromycin antibody. For normalization to total protein, the same Western blots were stained with the Swift Membrane Stain™ kit (G-Biosciences).

Statistics—Data are presented as mean ± S.E. Statistical analyses of two groups were performed as with Student's t test. $p < 0.05$ was considered statistically significant: *, $p < 0.05$; **, $p < 0.01$; ***, $p < 0.001$.

RESULTS

The Effects of FKBP12 Deficiency, Rapamycin, and SLF on Muscle Function—To determine whether reducing the interaction of FKBP12 with its targets in skeletal muscle contributes to the functional effects of rapamycin, we used three approaches to decrease the FKBP12 interactions without directly inhibiting mTORC1: 1) decreased skeletal muscle FKBP12 expression, 2) low doses of rapamycin, and 3) a drug (SLF) that displaces FKBP12 from RyR1 and other targets without inhibiting mTORC1 or calcineurin.

We created mice with a general knockout of FKBP12 (25), but the homozygous mice (FKBP12$^{null/null}$) died at birth from cardiac failure and/or respiratory insufficiency. Heterozygous FKBP12$^{WT/null}$ mice thrived and closely resembled the wild type (WT) and CRE$^+$ mice in our assays. We also created two strains of mice with deficiencies in FKBP12 in skeletal muscle (23). One strain of mice was homozygous for the floxed allele (FKBP12$^{lox/lox}$), and the second was heterozygous for the floxed allele and null for the second FKBP12 allele (FKBP12$^{lox/null}$, obtained by crossing FKBP12$^{lox/lox}$ with FKBP12$^{WT/null}$ mice). Both types of mice (FKBP12$^{lox/lox}$ and FKBP12$^{lox/null}$) expressed CRE$^+$ recombinase under the creatine kinase promoter and are on a C57BL6/J background. The magnitude of the muscle decrease in FKBP12 is shown in Fig. 1*A*. FKBP12 was decreased by 80–90% in most muscles of both types of FKBP12

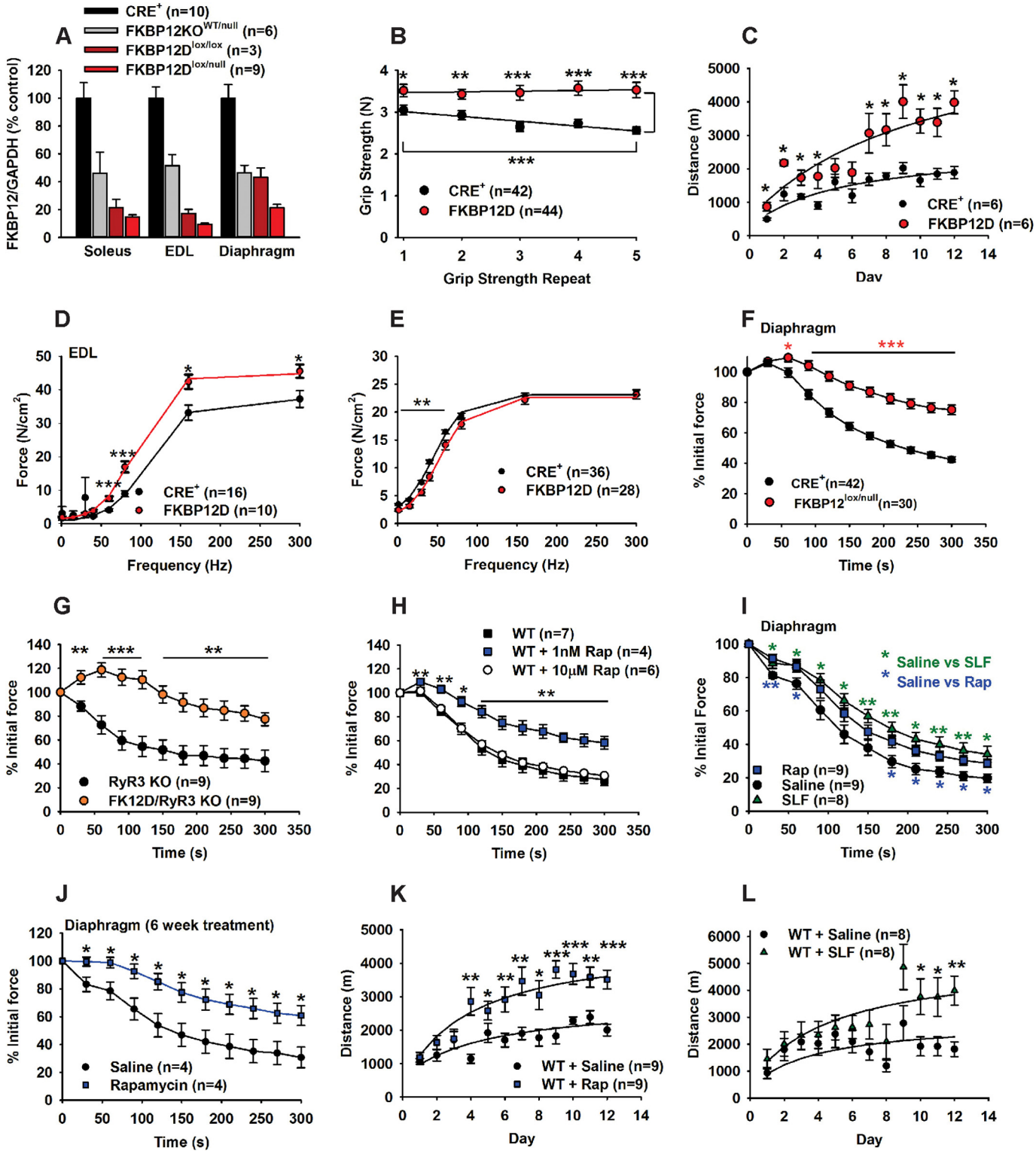

FIGURE 1. **Phenotype of mice with skeletal muscle FKBP12 deficiency.** *A*, levels of FKBP12 in muscle of CRE$^+$, FKBPP12$^{WT/null}$, FKBP12D$^{lox/lox}$, and FKBP12$^{lox/null}$ mice. *B*, grip strength of the four mouse paws, measured in five consecutive repeats. *C*, endurance running. CRE$^+$ and FKBP12D mice were run to exhaustion repeatedly for 12 consecutive days, and total distance run per day was determined. *D*, force-frequency curve for the EDL of CRE$^+$ and FKBP12D mice. *E*, force-frequency curve for the diaphragm muscle of CRE$^+$ and FKBP12D mice. *F*, diaphragm fatigue of CRE$^+$ and FKBP12D mice. *G*, diaphragm fatigue in mice that do not express RyR3 with and without FKBP12 deficiency. *H*, effect of rapamycin treatment on diaphragm fatigue *in vitro*. WT mice were sacrificed, and diaphragms were isolated. 1 nM or 10 μM rapamycin was added, and after 20 min, the force frequency and fatigue studies were performed. *I*, diaphragm fatigue in mice treated for 2 weeks with low dose rapamycin or SLF. *J*, diaphragm fatigue in mice treated for 6 weeks with low dose rapamycin. *K*, endurance running of mice treated with rapamycin. WT mice were injected with saline or rapamycin (10 μg/kg body weight), every other day, 1 h prior to test and run to exhaustion repeatedly for 12 consecutive days. Distance run each day is shown. *L*, endurance running of mice treated with SLF. WT mice were injected with saline or SLF (1 μg/kg body weight), every other day, 1 h prior to test and run to exhaustion repeatedly for 12 consecutive days. Distance run each day is shown. Data are shown as mean ± S.E. (*error bars*). *, $p < 0.05$; **, $p < 0.01$; ***, $p < 0.001$.

knockdown mice except in the diaphragms of the FKBP12$^{lox/lox}$ mice, where the decrease was less than in other muscles and less than in the diaphragms of the FKBP12$^{lox/null}$ mice. For the remainder of this paper, we present the data obtained with the FKBP12$^{lox/null}$ mice because the extent of knockdown of FKBP12 was greater across all muscle groups, the functional consequences of FKBP12 deficiency for muscle function were greater, and the FKBP12 levels varied less in the diaphragm among the FKBP12-deficient mice. For simplicity, these FKBP12$^{lox/null}$ mice are designated FKBP12D.

When compared with the CRE$^+$ mice, the FKBP12D mice had improved grip strength, which did not decline with repetitive trials (Fig. 1*B*) and increased running endurance (Fig. 1*C*). We have previously reported that these mice also display improved muscle recovery from injury (26). Overall, our data suggest that muscle function is greatly improved by FKBP12 deficiency. The data in Fig. 1, *B* and *C*, suggest that fatigue may be less in the FKBP12D mice.

Previous studies with FKBP12D on a mixed background showed small changes in the force-frequency curves (23) that were different from those obtained with muscles from FKBP12D mice back-crossed onto a clean C57B6/J background. With the mice on the C57B6J background, we found no differences in the force frequency curves in the soleus (data not shown), but the EDL of FKBP12D mice generated more force than the corresponding EDL muscles of CRE$^+$ mice, and the half-maximal stimulation frequency was shifted to the left by 17 Hz ($p < 0.001$) (Fig. 1*D*). The force-frequency curve for the diaphragm of FKBP12D displayed a 12-Hz rightward shift ($p = 0.001$) (Fig. 1*E*).

Although we found small but significant slowing of fatigue in the EDL and soleus muscle (data not shown), the most significant effects of FKBP12 deficiency on fatigue were found in the diaphragm (Fig. 1*F*). This slowing of diaphragm fatigue by FKBP12 deficiency was not dependent on the presence of a second isoform of RyR known to be expressed in diaphragm, RyR3, because the slowed fatigue was detected in diaphragms of mice that were deficient in both FKBP12 and RyR3 (Fig. 1*G*).

The finding that FKBP12 deficiency slows muscle fatigue raises the question of whether rapamycin and SLF can also slow fatigue. We tested the effects of rapamycin at two different concentrations on muscle fatigue in WT diaphragms. Treatment of isolated WT diaphragms with 1 nM rapamycin slowed diaphragm fatigue (Fig. 1*H*). In contrast, a high dose of rapamycin (10 μM, a concentration that should remove most of the FKBP12 from RyR1) did not slow diaphragm fatigue *in vitro* (Fig. 1*H*), suggesting that some drug-free FKBP12 is required to slow fatigue.

We also tested the effects of *in vivo* treatment of mice with low dose rapamycin and SLF. WT mice were injected (intreperitoneally) with rapamycin (10 μg/kg) or SLF (1 μg/kg) every other day for 2 weeks. The rapamycin dose used in this study was 50–1000-fold less than that used in mouse studies to inhibit mTORC1 signaling or promote longevity (0.5–10 mg/kg) (27–30). We found that diaphragm fatigue was also slowed by *in vivo* treatment with rapamycin and SLF (Fig. 1*I*). We also tested rapamycin (10 μg/kg every second day) for 6 weeks and found that again diaphragm fatigue was slowed (Fig. 1*J*).

The ability of low dose rapamycin to slow muscle fatigue led us to test *in vivo* low dose rapamycin on endurance running of the mice. We injected (intraperitoneally) mice with rapamycin (10 μg/kg) or SLF (1 μg/kg) every other day for 2 weeks. Consistent with the data obtained with FKBP12D mice, both rapamycin (Fig. 1*K*) and SLF (Fig. 1*L*) improved endurance running. The difference between rapamycin- and saline-treated mice was significant after only two treatments (day 4) and continued to improve during the 12 days of treatment (Fig. 1*K*).

A concern in the use of rapamycin to slow skeletal muscle fatigue is that, even at low doses, rapamycin could negatively impact cardiac muscle function. We found, using echocardiography, that cardiac function was not altered by rapamycin in mice treated for up to 4 weeks (Fig. 2).

The Effects of FKBP12 Deficiency, Rapamycin, and SLF on Fiber Type Distribution—Slowing of muscle fatigue is frequently associated with increases in oxidative fibers. Using myosin heavy chain (MHC) immunohistochemical staining, we found that FKBP12 deficiency and, to a lesser extent, rapamycin and SLF (2-week treatment) activated the slow fiber program to increase oxidative fibers in the diaphragm (Fig. 3, *A*, *D*, and *G*), soleus (Fig. 3, *B*, *E*, and *H*), and EDL (Fig. 3, *C*, *F*, and *I*) compared with control mice.

Effects of Rapamycin, SLF, and FKBP12 Deficiency on Muscle Ca^{2+} Handling—The slowing of muscle fatigue driven by FKBP12 deficiency or low dose rapamycin/SLF could be secondary to changes in intracellular Ca^{2+} handling. FKBP12 regulates the activity of the Ca^{2+} release channel, RyR1, by stabilizing the closed state of the channel, and drugs that completely remove FKBP12 from RyR1 increase SR Ca^{2+} leak (31). To evaluate effects of FKBP12 deficiency and low dose rapamycin and SLF on intracellular Ca^{2+} handling, we used either Fura 2 or Mag-Fluo 4 (loaded into fibers at room temperature; see "Ca^{2+} Measurements") to assess changes in cytosolic Ca^{2+} concentrations, Ca^{2+} transients, and the rate of return of Ca^{2+} poststimulation to baseline. In a single twitch (1 Hz), the rate of return of cytosolic Ca^{2+} to baseline was slower in FKBP12D fibers than in CRE$^+$ fibers (Fig. 4*A*). This could have reflected slowed reuptake of Ca^{2+} into the SR, increased Ca^{2+} influx, or decreased cytosolic Ca^{2+} buffering. With repetitive 50-Hz trains (representative transients shown in Fig. 4*B*), both the poststimulation cytosolic Ca^{2+} (Fig. 4*C*) and the peak amplitude of the Ca^{2+} transient (Fig. 4*D*) increased in FKBP12D compared with CRE$^+$ fibers, suggesting enhanced rather than decreased refilling of SR Ca^{2+} stores and a possible net gain of Ca^{2+} to the fiber. Although Ca^{2+} enters the fiber during stimulation primarily through the voltage-gated Ca^{2+} channel, $Ca_V1.1$, this channel shuts down immediately following stimulation.

In response to repetitive tetanic (100-Hz) stimulation, the Ca^{2+} transient amplitude declined more slowly in FKBP12D compared with CRE$^+$ fibers (Fig. 4*E*). Similar results were obtained with 10 nM rapamycin and 1 nM SLF in fibers from WT mice (Fig. 4, *F* and *G*). Poststimulation 4-chloro-*m*-cresol (4CmC) releasable Ca^{2+} stores (Fig. 4*H*) were higher in fibers from FKBP12D compared with CRE$^+$ mice and in SLF- and

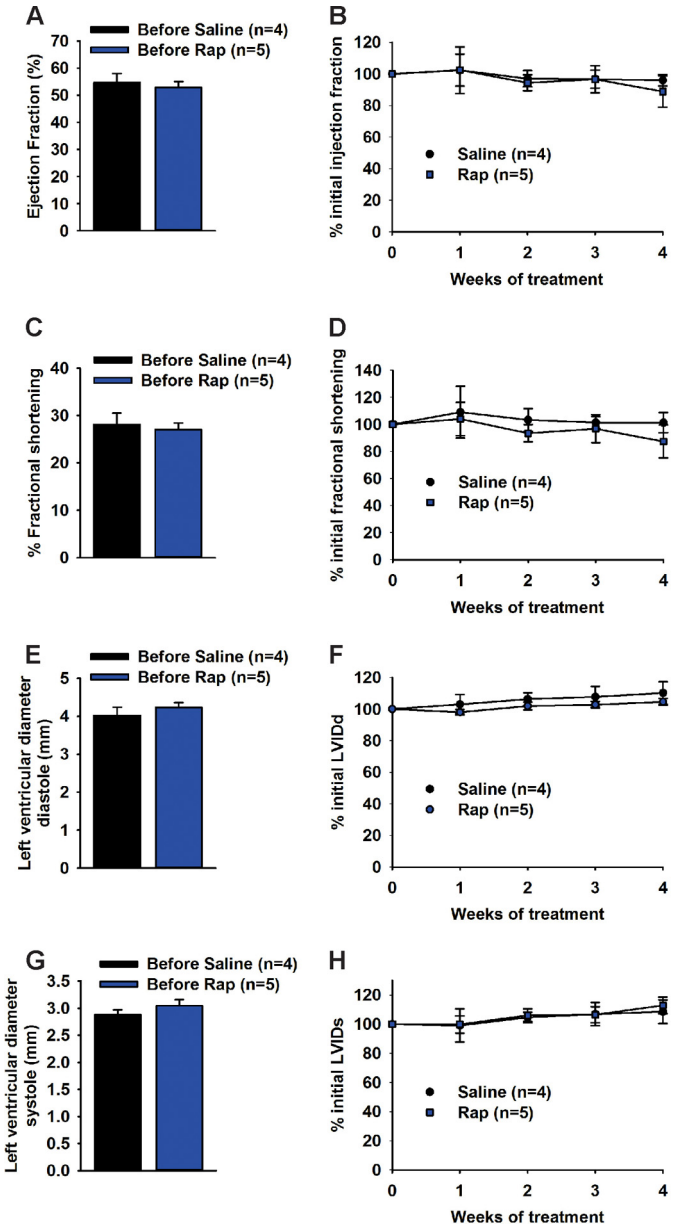

FIGURE 2. **Effects of low dose rapamycin on cardiac function.** 6–8-week-old C57/Bl6J mice were treated for 4 weeks with rapamycin (10 μg/kg), and cardiac function was measured using echocardiography once per week. *A*, average ejection fraction before rapamycin treatment. *B*, ejection fraction over time as a percentage of the initial measurement. *C*, average fractional shortening before rapamycin treatment. *D*, fractional shortening over time as a percentage of the initial measurement. *E*, average left ventricular internal diameter at diastole before rapamycin treatment. *F*, left ventricular internal diameter at diastole over time as a percentage of the initial measurement. *G*, average left ventricular internal diameter at systole before rapamycin treatment. *H*, left ventricular internal diameter at systole over time as a percentage of the initial measurement. Data are shown as mean ± S.E. (*error bars*).

rapamycin-treated compared with untreated fibers from WT mice. Increased SR Ca^{2+} stores and diminished decline of Ca^{2+} transients with repetitive fatiguing stimulation again suggested a net increase of Ca^{2+} in the fibers. To explore this possibility, we used a manganese quench assay to assess changes in Ca^{2+} influx into the fiber. Electrically stimulated Ca^{2+} influx into FDB fibers was enhanced by SLF, rapamycin, and FKBP12 deficiency (*manganese quench curves* in Fig. 4, *I–K*, and *slopes* in Fig. 4*L*).

These data suggest that the drugs and FKBP12 deficiency are enhancing the opening of a Ca^{2+} influx pathway during electrical stimulation. The most obvious possibility is $Ca_V1.1$, the voltage-dependent Ca^{2+} channel that mechanically gates RyR1 opening, but channels activated subsequent to excitation-contraction coupling may also contribute. Both enhanced refilling of SR Ca^{2+} stores and increased oxidative fibers are likely to underlie the improved endurance of the FKBP12-deficient and the SLF/rapamycin-treated mice. In addition, changes in the amplitude of the Ca^{2+} transient and the poststimulation cytosolic Ca^{2+} concentrations impact other pathways that respond to alterations in the amplitude, duration, and location of Ca^{2+} signals.

Estimation of the Effects of FKBP12 Deficiency on the FKBP12-RyR1 Interaction—Although FKBP12 has other targets in skeletal muscle (*e.g.* TGFβR1, Ras), little is known about the affinity of these proteins for FKBP12. The most abundant FKBP12-binding protein in skeletal muscle is RyR1. Complete removal of FKBP12 from RyR1 induces SR Ca^{2+} leak (32); however, no assessment of effects on intracellular Ca^{2+} regulation of partial removal of FKBP12 from RyR1 has been performed. We estimated the effects of FKBP12 deficiency on the FKBP12-RyR1 interaction (see complete description of the approach under "Materials and Methods"). Using Western blotting and purified FKBP12 to generate a standard curve (Fig. 5, *A* and *B*), we calculated the total concentration of FKBP12 in the soleus, EDL, and diaphragms of CRE^+ mice to be 1.6 ± 0.3, 1.3 ± 0.2, and 3.0 ± 0.5 μM ($n = 7$), respectively. In FKBP12D mice, the total FKBP12 concentrations in the soleus, EDL, and diaphragm were calculated to be 0.1 ± 0.06, 0.08 ± 0.02, and 0.37 ± 0.07 μM ($n = 7$), respectively. The concentration of FKBP12 binding sites on RyR1 (four FKBP12 binding sites per RyR1 tetramer) was between 200 and 400 nM, and the affinity of FKBP12 for RyR1 was 8–30 nM, depending on temperature (Fig. 5, *C* and *D*). There is adequate FKBP12 in CRE^+ muscle to saturate >95% of the binding sites on RyR1, and, despite a 80–90% decrease in FKBP12 levels in the FKBP12D muscle, there is adequate FKBP12 in FKBP12D muscle to decrease its interaction with RyR1 by less than 50% in most muscles. RyR1 protein levels tended to decrease in FKBP12 diaphragm (Fig. 5, *E* and *F*), but RyR1 mRNA levels were unchanged (Fig. 5*H*). $Ca_V1.1$ protein levels (Fig. 5, *E* and *G*) and mRNA (Fig. 5*I*) were not altered by FKBP12 deficiency. Neither RyR1 oxidation nor phospho-Ser-2844 phosphorylation is altered by FKBP12 deficiency (data not shown).

Other Ca^{2+}-handling Proteins—Changes in SR Ca^{2+} stores could arise from secondary changes in the proteins that regulate SR Ca^{2+} release, SR Ca^{2+} uptake, or SR Ca^{2+} buffering. FKBP12.6, another immunophilin that binds and modulates RyR1 was present in skeletal muscle at levels below the detection with our antibodies, but the mRNA levels for FKBP12.6 were not altered in the FKBP12D muscle (Fig. 6*A*). Western blots for the sarcoplasmic reticulum/endoplasmic reticulum Ca^{2+}-ATPase 1 (SERCA1), SERCA2, and calsequestrin (CSQ) are shown in Fig. 6*B*. Consistent with the increase in percentage of type I fibers, SERCA1 (found in type II fibers) protein levels were decreased in the muscle FKBP12D mice (Fig. 6*C*). SERCA2 protein levels were increased in the soleus and the diaphragm of the FKBP12 mice (Fig. 6*D*). Calsequestrin 1 and 2

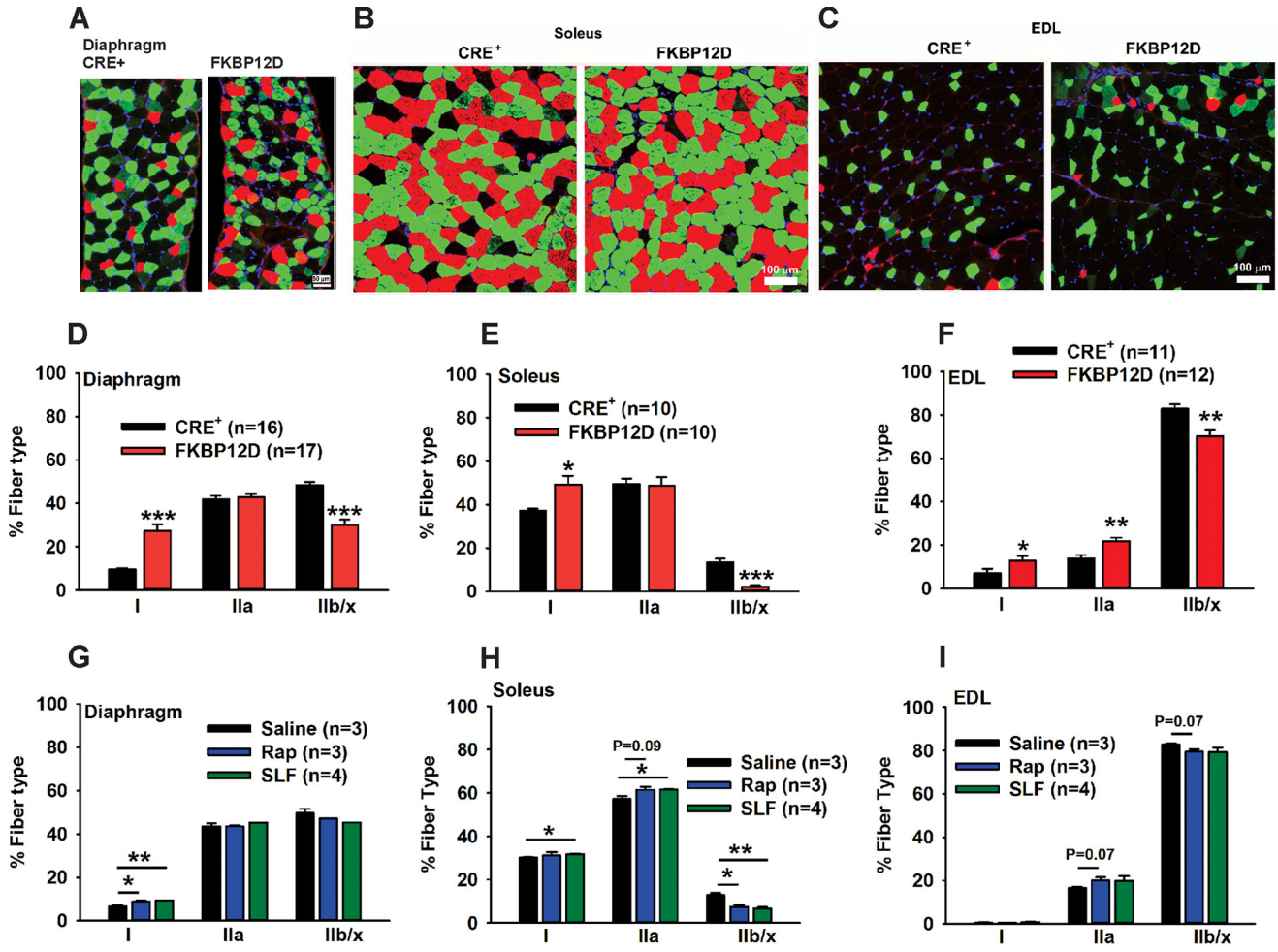

FIGURE 3. **Effect of FKBP12 deficiency and low dose rapamycin and SLF on fiber type distribution.** *A*, MHC fiber type staining in CRE$^+$ and FKBP12D diaphragms by MHC immunocytochemistry. Type I fibers are *pseudocolored red*. Type IIa fibers are *pseudocolored green*, and type IIb/x fibers are *black*. Mice were 7–9 weeks old. *B*, MHC fiber type staining in CRE$^+$ and FKBP12D soleus by MHC immunocytochemistry. *C*, MHC fiber type staining in CRE$^+$ and FKBP12D EDL by MHC immunocytochemistry. *D*, fiber type distribution in the diaphragm of FKBP12D and CRE$^+$ mice. *E*, fiber type distribution in the soleus of FKBP12D and CRE$^+$ mice. *F*, fiber type distribution in the EDL of FKBP12D and CRE$^+$ mice. *G*, analysis of diaphragm fiber type changes after low dose rapamycin or SLF. WT mice were injected with saline, rapamycin (10 μg/kg body weight), or SLF (1 μg/kg body weight) every other day. At the end of 2 weeks, mice were sacrificed, and muscles were isolated and sectioned with a cryostat for staining with MHC antibodies. Mice were 8–11 weeks of age. *H*, analysis of soleus fiber type changes after low dose rapamycin or SLF. *I*, analysis of EDL fiber type changes after low dose rapamycin or SLF. Data in the figure are shown as mean ± S.E. (*error bars*). *, $p < 0.05$; **, $p < 0.01$; ***, $p < 0.001$.

(CSQ1/2), which binds Ca^{2+} in the luminal SR, is increased in the soleus of FKBP12D mice, but CSQ1/2 levels were not statistically different in the EDL or diaphragm (Fig. 6*E*).

FKBP12 Deficiency and Rapamycin Increase Protein Synthesis—Given that rapamycin is a known inhibitor of mTORC1 and, hence, protein synthesis in mice at doses between 2 and 10 mg/kg, we assessed the effects of low dose (10 μg/kg) rapamycin, SLF (1 μg/kg), and FKBP12 deficiency on protein synthesis using a modified SUnSET assay (33). To minimize variations in protein synthesis associated with variations in time of food intake, we deprived mice (CRE$^+$, FKBP12D, and WT) of food for 6 h, followed by a single intraperitoneal injection with saline, rapamycin, or SLF, and then food was provided for 2 h prior to sacrifice. The mice were injected with puromycin 35 min before the sacrifice. FKBP12 deficiency (Fig. 7, *A* and *B*) and low dose rapamycin and SLF treatment (Fig. 7, *C* and *D*) increased protein synthesis.

An increase, rather than a decrease, in protein synthesis suggests that at a low dose, rapamycin is activating rather than inhibiting mTORC1. We assessed the effects of FKBP12 deficiency, low dose rapamycin, and SLF on signal transduction pathways both upstream (phospho-Akt (Ser-473)/Akt and phospho-Akt (Thr-308)/Akt) and downstream of mTORC1 (phospho-S6 (Ser-235/Ser236), T46-4EBP14E-BP1 (Thr-37/Thr-46)/4E-BP1, and phospho-eEF2 (Thr-56)/eEF2) that modulate the rate of protein synthesis. We also assessed the status of MAPK signaling by analyzing phospho-ERK/ERK and ribosome levels (also regulated by mTORC1) by examining the levels of L7a normalized to GAPDH. Note that all data are normalized to the Western blot values for the WT or CRE$^+$ controls from the same Western blot, which allowed us to do multiple replicates (each normalized to their own controls) to ensure significance. For the drug treatments, mice were given a single dose of either rapamycin or SLF, and signal transduction changes were assessed after 2 h. Mice were sacrificed 2 h after administration of the drugs.

Mice (either FKBP12D (Fig. 8, *A–D*) or treated for 2 h (Fig. 8, *E–H*) or 2 weeks (Fig. 8, *I–L*) with low dose rapamycin or SLF) displayed pronounced increases in both phospho-S6 (Ser-235/

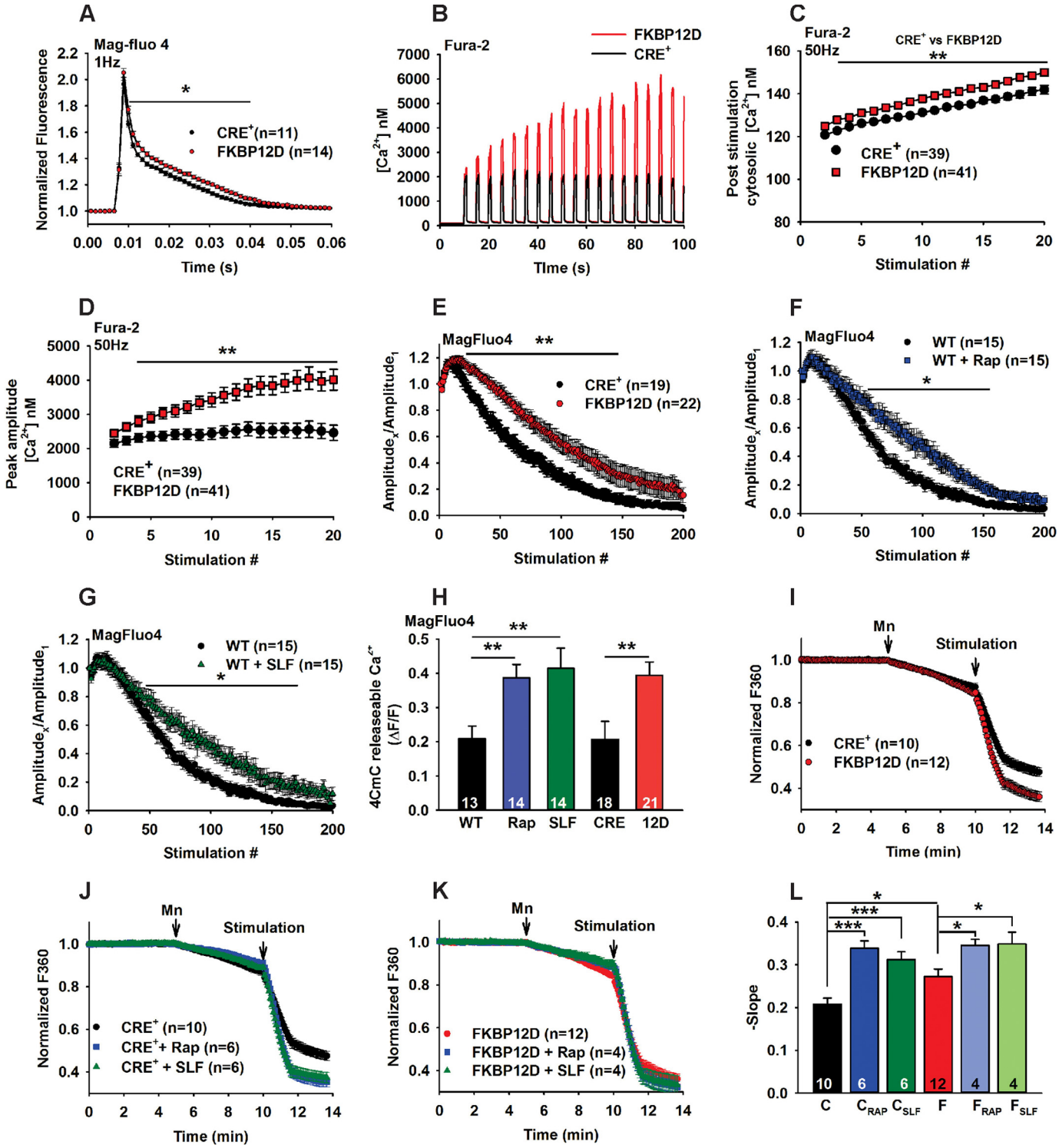

FIGURE 4. **Effect of FKBP12 deficiency, rapamycin and SLF on Ca^{2+} handling in FDB fibers.** *A*, effect of FKBP12 deficiency on the Ca^{2+} transient assessed with Mag-fluo4 fluorescence elicited by a single twitch stimulation (1 Hz). *B*, the effect of FKBP12 deficiency on the amplitude of the Ca^{2+} transients during repetitive 50-Hz fatiguing stimulation assessed with Fura-2. *C*, post-transient Ca^{2+} concentrations in fibers stimulated as described in *B*. *D*, analysis of the amplitude of the Ca^{2+} transients with repetitive stimulation. *E*, effects of fatiguing stimulation (100 Hz) on the amplitude of the Ca^{2+} transients in CRE^+ and FKBP12D fibers measured with Mag-fluo-4. *F*, effects of fatiguing stimulation on the amplitude of the Ca^{2+} transients in WT fibers treated with rapamycin and measured with Mag-fluo-4. *G*, effects of fatiguing stimulation on the amplitude of the Ca^{2+} transients in WT fibers treated with SLF and measured with Mag-fluo-4. Note that the *control curve* is the same as in *F* because SLF and rapamycin were each tested with each fiber preparation. *H*, 4-chloro-*m*-cresol (*4CmC*)-releasable Ca^{2+} measured immediately after the fatiguing stimulation of CRE^+ and FKBP12 or in WT fibers treated with low dose rapamycin or SLF. *I*, manganese quench and the effects of stimulation in fibers from CRE^+ and FKBP12D mice. *J*, manganese quench and the effects of stimulation in fibers treated with rapamycin or SLF from CRE^+ control mice. *K*, manganese quench and the effects of stimulation in fibers treated with rapamycin or SLF from FKBP12D mice. *L*, manganese quench slopes during stimulation and effects of rapamycin, SLF, and FKBP12 deficiency. *C*, CRE^+; *F*, FKBP12D. Data are shown as mean ± S.E. (*error bars*). *, $p < 0.05$; **, $p < 0.01$; ***, $p < 0.001$.

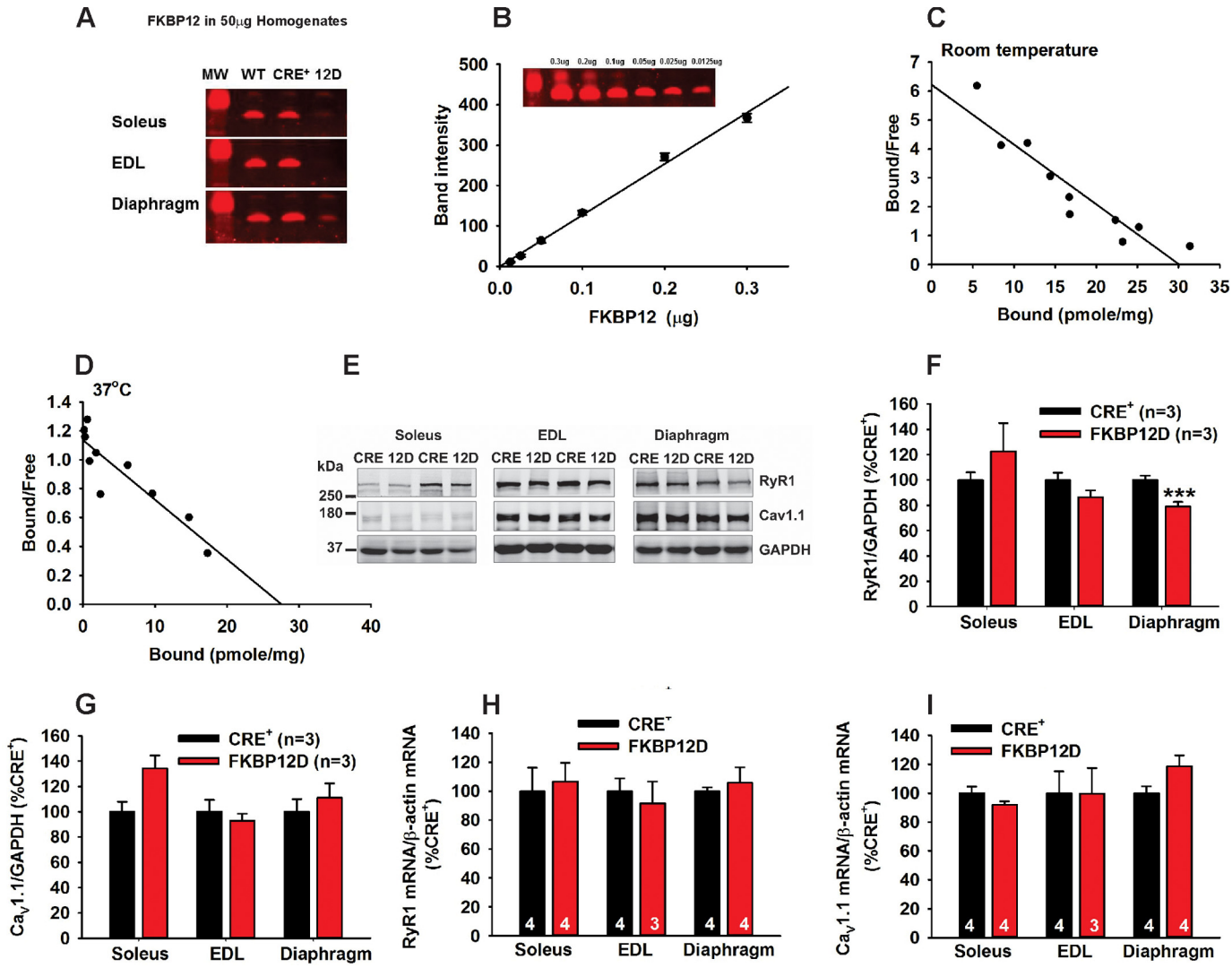

FIGURE 5. **Analysis FKBP12, RyR1, and $Ca_V1.1$ levels in FKBP12D and CRE^+ mice.** *A*, FKBP12 in homogenates. *B*, FKBP12 standard curve. *C*, Scatchard analysis of [^{35}S]FKBP12 binding at room temperature to muscle membranes from WT mice. *D*, Scatchard analysis of [^{35}S]FKBP12 binding at 37 °C to muscle membranes from WT mice. *E*, Western blots for $Ca_V1.1$, RyR1, and GAPDH in muscles of 7-week-old FKBP12D and CRE^+ mice. *F*, analysis of RyR1 protein normalized to GAPDH in soleus, EDL, and diaphragm of CRE^+ and FKBP12D mice. *G*, analysis of $Ca_V1.1$ normalized to GAPDH in FKBP12D and CRE^+ soleus, EDL, and diaphragm. *H*, RyR1 mRNA from quantitative RT-PCR. *I*, CaV1.1 mRNA from quantitative RT-PCR. Data are shown as mean ± S.E. (*error bars*).

Ser-236)/S6 and 4E-BP1 (Thr-37/Thr-46)/4E-BP1. We also found increases in phospho-Akt (Ser-474)/Akt, phospho-Akt (Thr-308)/Akt, phospho-ERK (Thr202/Tyr-204)/ERK/GAPDH, and L7a/GAPDH (a ribosomal protein marker). These findings demonstrate that FKBP12 deficiency, low dose rapamycin, and SLF all activate mTORC1, possibly upstream of Akt. The elevated phospho-Akt (Ser-473)/Akt and phospho-Akt (Thr-308)/Akt suggested that mTORC2 and the PI3K pathway activation led to downstream activation of mTORC1. However, the increased phosphorylation of ERK1/2 could have also contributed to the increases in phospho-S6 (Ser-235/Ser-236)/S6 and phospho-4E-BP1(Thr-37/Thr-46)/4E-BP1.

Although autophagy is also stimulated by mTORC1 activation, we did not find differences in beclin 1 or Atg5 levels in any muscle of the FKBP12D or rapamycin-treated mice (data not shown). We found a small increase in beclin 1 in the EDL muscle of SLF-treated mice but no change in Atg5 (data not shown). We conclude that autophagy is not activated by these treatments.

FKBP12 regulates TGFβR1 signaling, but other than a small increase in phospho-SMAD2 (Ser-465/Ser-467)/SMAD2 in the soleus after rapamycin treatment, we failed to detect any other changes in phospho-SMAD2 (Ser-465/Ser-467)/SMAD2 in muscles of FKBP12D mice or in mice treated with either rapamycin or SLF (data not shown), suggesting little change in TGFβ signaling.

Signal Transduction Pathways That Modulate Fiber Type Distribution—One of the major changes associated with the FKBP12D mice is an increase in type I fibers. We analyzed pathways known to regulate fiber type changes in the muscle (Fig. 9, *A–G*). We found no differences in the protein levels of ERRγ, a known contributor to the slow muscle program (34), in FKBP12D muscle compared with CRE^+ muscle (Fig. 9*B*). However, muscle levels of ERRα, which has many overlapping functions with ERRγ, enhances PGC-1α signaling (35), and is involved in muscle repair (36), were elevated in the muscle of FKBP12D mice (Fig. 9*C*). PPARβ/δ also contributes to the slow fiber program (19) and is elevated in the muscle of FKBP12D mice (Fig. 9*D*). Both ERRα and

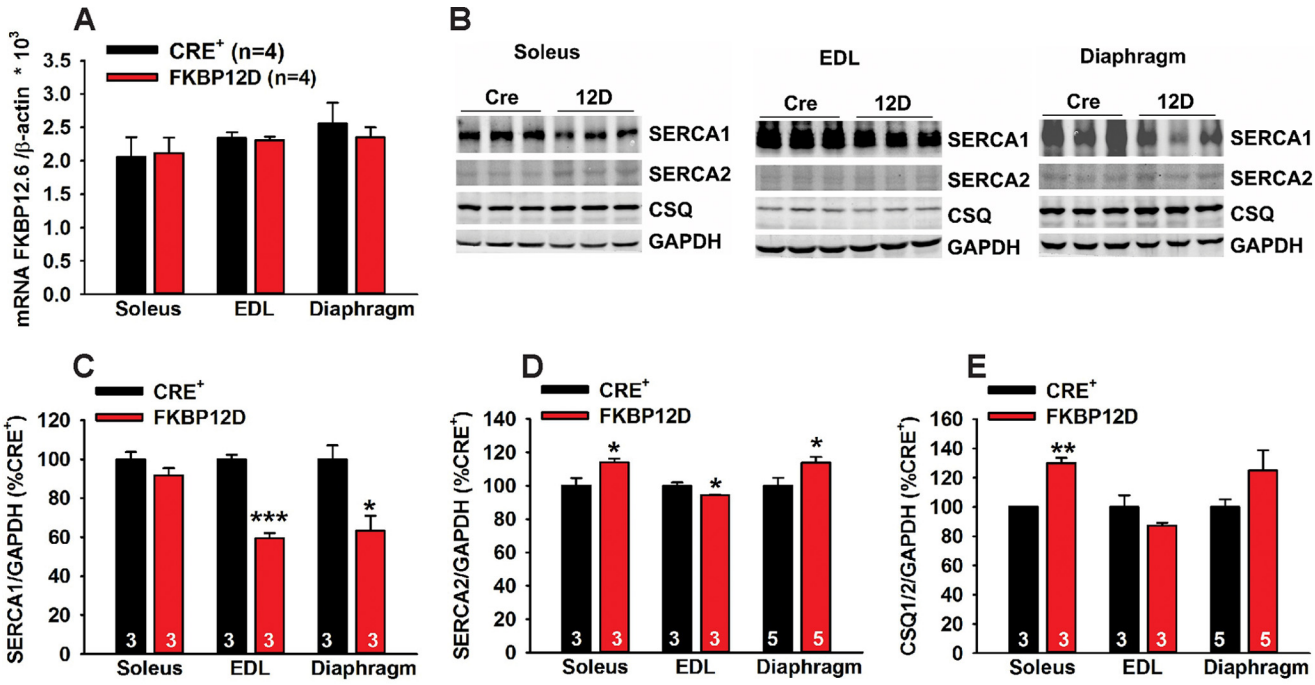

FIGURE 6. **Muscle levels of FKBP12.6, SERCA1, SERCA2, and calsequestrin.** *A*, mRNA for FKBP12.6 assessed by quantitative RT-PCR. FKBP12.6 protein levels are not detectable in skeletal muscle with the antibodies used. *B*, Western blots for SERCA1, SERCA2, and CSQ 1/2 (*CSQ*) in muscle of FKBP12D and CRE$^+$ mice. *C*, analysis of SERCA1 normalized to GAPDH and plotted as percentage of CRE$^+$. *D*, analysis of SERCA2 normalized to GAPDH and plotted as percentage of CRE$^+$. *E*, analysis of CSQ1/2 normalized to GAPDH and plotted as percentage of CRE$^+$. Data are shown as mean ± S.E. (*error bars*). *, $p < 0.05$; **, $p < 0.01$; ***, $p < 0.001$.

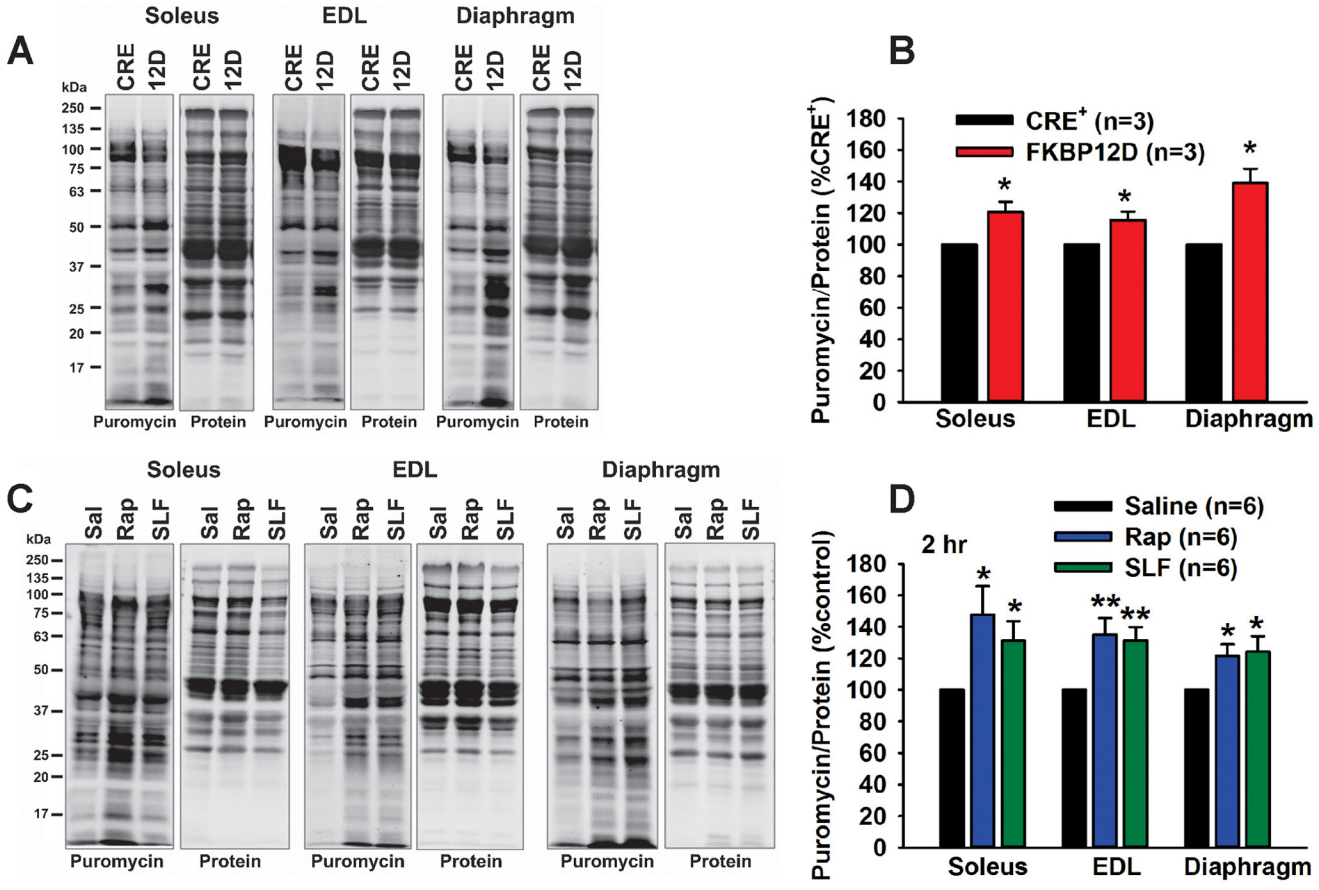

FIGURE 7. **Effects of FKBP12 deficiency and low dose rapamycin and SLF on protein synthesis.** *A*, Western blot for puromycin in muscle homogenates from CRE$^+$ and FKBP12D mice (6–8 weeks of age) after injection with puromycin as described under "Materials and Methods." Shown are both the Western blot for puromycin and the total protein stain. *B*, analysis of puromycin Western blots. *C*, Western blot for puromycin in mice treated with saline, rapamycin (10 μg/kg), or SLF (1 μg/kg). Mice (6–8 weeks of age) were injected with puromycin and sacrificed, muscle was isolated and homogenized, and the muscle lysates were used for Western blotting with anti-puromycin antibodies. *D*, analysis of puromycin Western blots. Data are shown as mean ± S.E. (*error bars*). *, $p < 0.05$; **, $p < 0.01$.

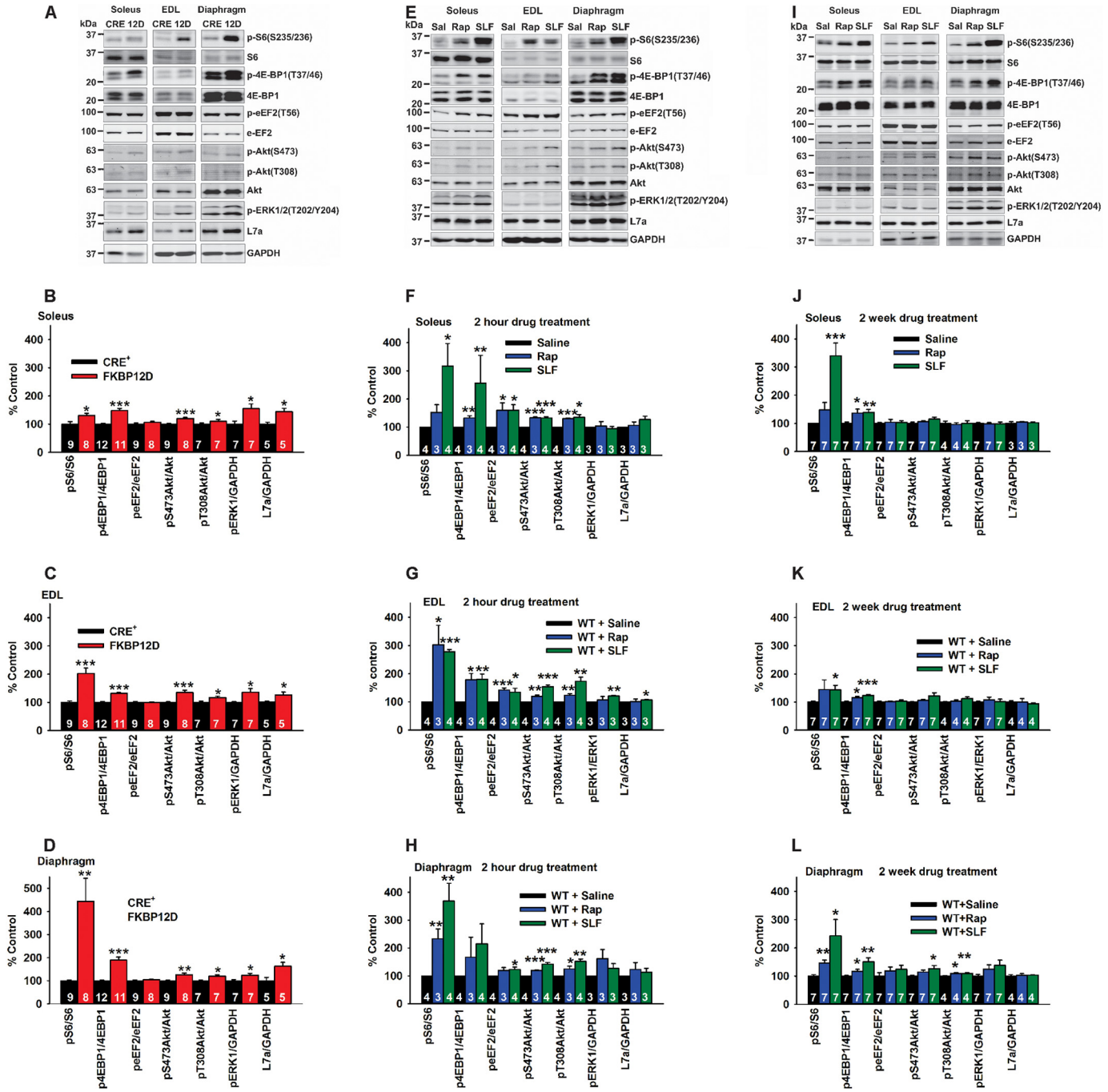

FIGURE 8. **Effects of FKBP12 deficiency and low dose rapamycin and SLF on signal transduction pathways that modulate protein synthesis.** *A*, representative Western blot of proteins that impact protein synthesis in FKBP12D and CRE$^+$ mice (8–10 weeks old). *B*, analysis of signal transduction changes in the solei of FKBP12D and CRE$^+$ mice. *C*, analysis of signal transduction changes in the EDLs of FKBP12D and CRE$^+$ mice. *D*, analysis of signal transduction changes in the diaphragms of FKBP12D and CRE$^+$ mice. *E*, representative Western blot for proteins that impact protein synthesis in muscle of mice treated with saline, rapamycin, or SLF for 2 h. *F*, analysis of signal transduction changes in the solei of saline-, rapamycin-, and SLF-treated mice. *G*, analysis of signal transduction changes in the EDLs of saline-, rapamycin-, and SLF-treated mice. *H*, analysis of signal transduction changes in the diaphragms of saline-, rapamycin-, and SLF-treated mice. *I*, representative Western blot for proteins that impact protein synthesis in muscle of mice treated with saline, rapamycin, or SLF for 2 weeks. *J*, analysis of signal transduction changes in the solei of mice treated with saline, rapamycin, or SLF for 2 weeks. *K*, analysis of signal transduction changes in the EDLs of mice treated with saline, rapamycin, or SLF for 2 weeks. *L*, analysis of signal transduction changes in the diaphragms of mice treated with saline, rapamycin, or SLF for 2 weeks. Data are shown as mean ± S.E. (*error bars*). *, $p < 0.05$; **, $p < 0.01$; ***, $p < 0.001$.

ERRγ mRNA levels were elevated in muscle of FKBP12D compared with CRE$^+$ mice (Fig. 9, *E* and *F*).

Calcineurin is thought to play a major role in fiber type changes in muscle, and we previously demonstrated an increase in calcineurin levels in FKBP12D mice (23). However, we were unable to detect differences in calcineurin activity between muscle homogenates of FKBP12D and CRE$^+$ mice (Fig. 9*G*). This does not preclude activation of calcineurin in muscle due to increases in Ca^{2+} because these changes cannot be assessed in the *in vitro* assay, where Ca^{2+} concentrations are controlled.

The fiber type changes that occurred after a 2-week treatment with SLF and rapamycin were small compared with those

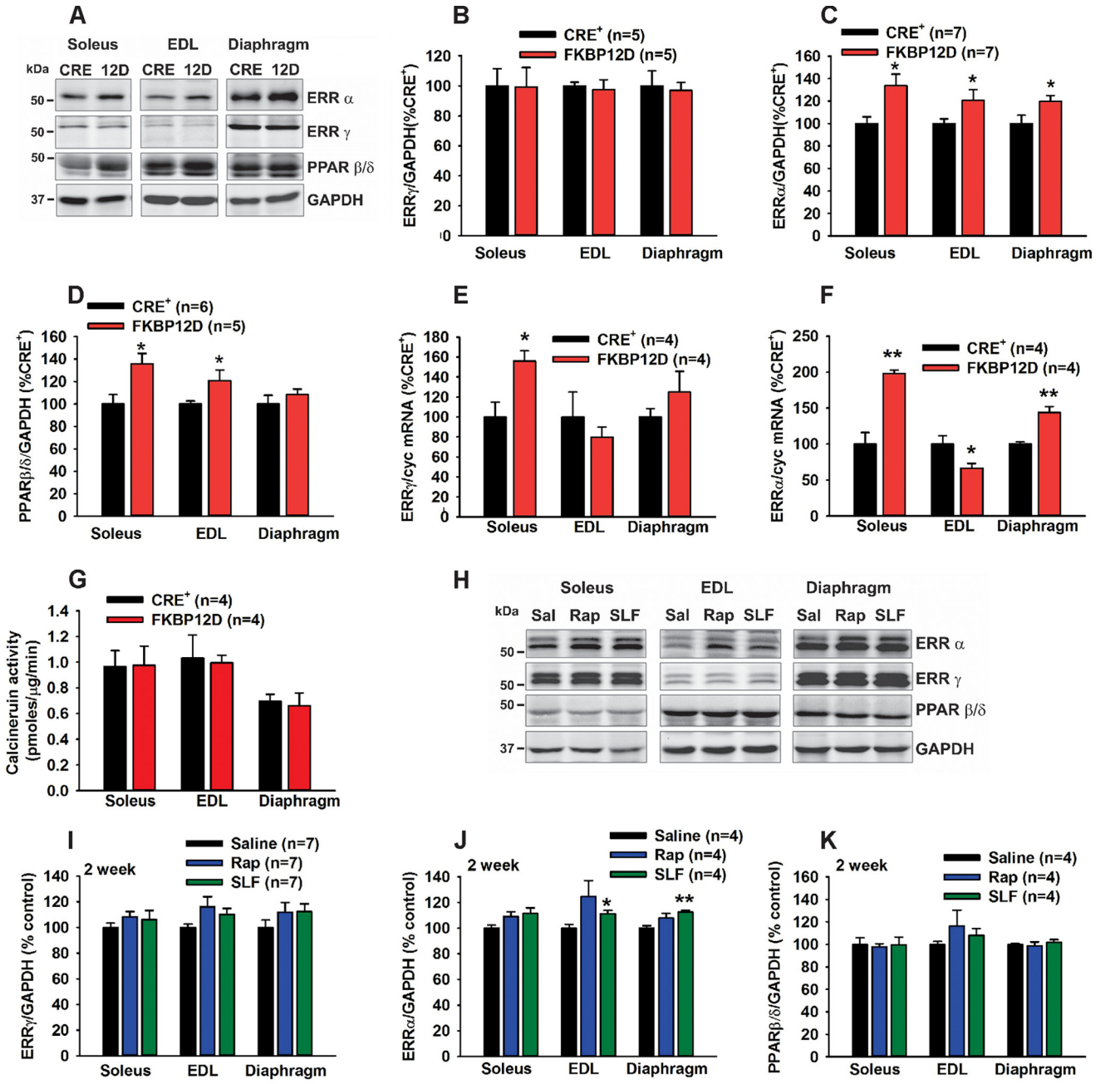

FIGURE 9. **Effect of FKBP12 deficiency, rapamycin, and SLF on pathways that regulate the slow fiber program.** *A*, Western blot for ERRα, ERRγ, PPARβ/δ, and GAPDH in muscles from FKBP12D and CRE$^+$ mice (8–10 weeks old). *B*, analysis of ERRγ levels. *C*, analysis of ERRα levels. *D*, analysis of PPARβ/δ levels. *E*, analysis of the effects of FKBP12 deficiency on the mRNA levels of ERRγ. *F*, analysis of the effects of FKBP12 deficiency on the mRNA levels of ERRα. *G*, calcineurin activity in muscles of CRE$^+$ and FKBP12D mice. *H*, Western blot for the effects of 2-week treatment with SLF and rapamycin on ERRα and ERRγ levels (8–10-week-old mice). *I*, analysis of ERRγ levels. *J*, analysis of ERRα levels. *K*, analysis of PPARβ/δ levels. Data are shown as mean ± S.E. (*error bars*). *, $p < 0.05$; **, $p < 0.01$.

seen in the muscle of FKBP12D mice. Not surprisingly, the changes in the proteins that drive the slow fiber program were also smaller (Fig. 9, *H–K*), and we only detected a significant difference in ERRα (Fig. 9*J*). No changes in these proteins were detected in mice treated for only 2 h with either rapamycin or SLF (data not shown).

DISCUSSION

In this paper, we explore the multiple roles of FKBP12 in skeletal muscle by examining the effects of FKBP12 deficiency and the drugs, rapamycin and SLF, that bind FKBP12. Most studies with rapamycin in mice use doses from 2 to 10 mg/kg body weight, doses often related to mTORC1 inhibition and decreased protein synthesis. In contrast, our data suggest that much lower concentrations of rapamycin (10 μg/kg) and the non-immunosuppressive FKBP ligand SLF (1 μg/kg) enhance refilling of SR Ca^{2+} stores to increase protein synthesis, slow muscle fatigue, and initiate up-regulation of type I fibers. A challenge when assessing the functional consequences of treatment with drugs such as rapamycin is to determine the specific

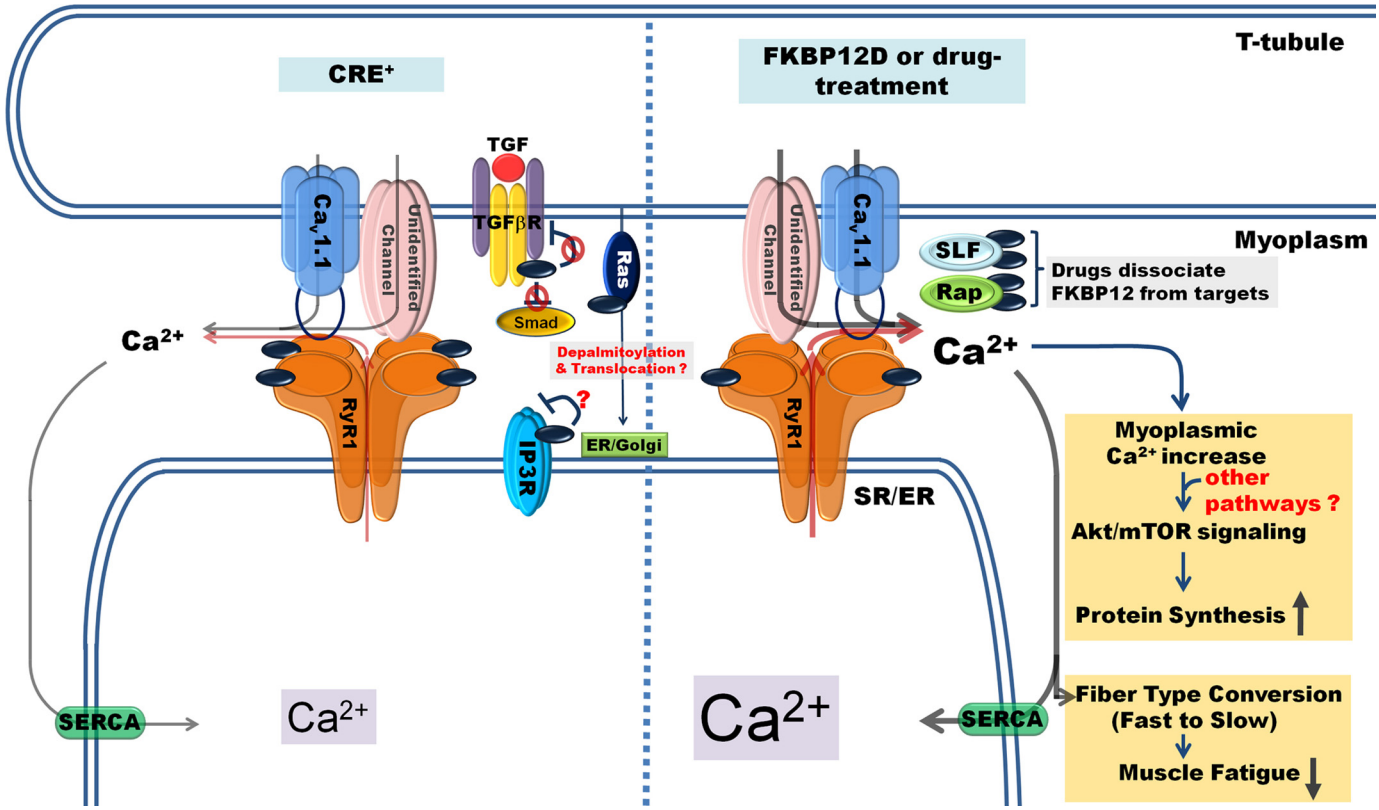

FIGURE 10. **A model for the effects of FKBP12 deficiency, low dose rapamycin, and SLF on muscle function.** We propose that depletion of FKBP12, low dose rapamycin, and SLF alter the conformation and/or Ca^{2+} leak via RyR1 and increase Ca^{2+} influx into the fiber. This added Ca^{2+} facilitates refilling of SR Ca^{2+} stores and prevents depletion during repetitive stimulation. Altered Ca^{2+} handling and/or other FKBP12 targets activate mTORC1 to increase protein synthesis and increases ERRα to activate the slow fiber program.

contributions of alterations in the multiple pathways regulated by FKBP12. We identify FKBP12-dependent changes in both myoplasmic Ca^{2+} handling and protein synthesis that are likely to impact multiple processes in the muscle fiber but found no changes in TGFβR1 signaling.

Both FKBP12 deficiency and low dose rapamycin and SLF improve skeletal muscle endurance, most likely due to the combined effects of enhanced refilling of SR Ca^{2+} stores (thereby slowing depletion with repetitive stimulation) and increased fatigue-resistant type I fibers, because both of these parameter are known to modulate muscle fatigue (18–21). Consistent with an increase in type I fibers, ERRα and PPARβ/δ are increased by FKBP12 deficiency and 2-week treatment with rapamycin and SLF. We detect small increases in the mRNA for ERRγ but no apparent changes in ERRγ protein levels. However, the possibility exists that changes in Ca^{2+} handling impact this signaling pathway because ERRγ has a predicted Ca^{2+} calmodulin binding site (see the Calmodulin Target Database Web site).

Low dose rapamycin (10 nM for a 1-h incubation with isolated muscle prior to the fatiguing protocol) also slows muscle fatigue in isolated diaphragm fibers, suggesting that, although the increase in type I fibers contributes to improved endurance, the fiber type changes are not required for slowing of muscle fatigue.

The major changes in Ca^{2+} handling in adult muscle fibers in response to low dose rapamycin, low dose SLF, or FKBP12 deficiency were increased Ca^{2+} influx, increased cytosolic Ca^{2+} concentrations, increased SR Ca^{2+} stores, and increased SR Ca^{2+} release. Previously, using myotubes, we found that FKBP12 deficiency increased voltage-gated Ca^{2+} influx but decreased SR Ca^{2+} release (23). The difference in SR Ca^{2+} release between myofibers and myotubes may reflect the lack of structural organization in myotubes (37) and/or differences in the expression levels of CRE^{+} recombinase and, hence, the efficiency of the knockdown of FKBP12 expression. Because our objective in this study was to assess the functional consequences of low dose rapamycin or SLF and FKBP12 deficiency for the function of adult skeletal muscle, all studies in this paper were performed with adult muscle fibers. Because the increased influx required electrical stimulation, the most likely candidate for mediating the Ca^{2+} influx is the voltage-dependent Ca^{2+} channel, $Ca_V1.1$. However, given the small magnitude of the Ca^{2+} current through $Ca_V1.1$ and its inactivation (38), it seems unlikely that $Ca_V1.1$ alone is responsible for the increased Ca^{2+} influx and enhanced Ca^{2+} store refilling, especially poststimulation (Fig. 4*A*). Additional channels that contribute to this influx remain to be identified. Regardless of whether the Ca^{2+} influx is due entirely to altered $Ca_V1.1$ or another Ca^{2+} channel, the increased Ca^{2+} influx to the muscle is likely to underlie the enhanced Ca^{2+} store refilling.

Bellinger *et al.* (31) found that FKBP12 association with RyR1 is reduced following a single bout of swimming exercise in mice. This effect was dose-dependent, increasing with increasing duration of exercise. In addition, with chronic (3 weeks) swim training, RyR1 *S*-nitrosylation increased, whereas FKBP12

association with RyR1 decreased. In this study, the effect of the swim training program on fatigue was measured using an entirely different mode of exercise (treadmill running), making assessment of the effects of the training program on endurance and fatigue difficult at best. When mice or humans are tested using the mode of exercise for which they have trained, adaptation typically occurs very rapidly. Thus, an alternative interpretation of the results of Bellinger *et al.* (31) is that RyR1 *S*-nitrosylation of RyR1 is part of the normal adaptation to endurance exercise training. The fatigue-slowing effects observed by Bellinger *et al.* (31) were also very small, and the drug used (S107) interacts with RyR1 to increase FKBP12 binding and slow passive SR Ca^{2+} leak. Our data suggest that low dose rapamycin (used clinically at much higher doses that we are using) and SLF interact with FKBP12 to alter the interaction of RyR1 with a Ca^{2+} influx channel. The effects of low dose rapamycin and SLF are both activity-dependent and transient and do not lead to sustained increases in cytosolic Ca^{2+}. The transient Ca^{2+} changes are beneficial rather than detrimental because Ca^{2+} influx enhances the refilling of SR Ca^{2+} stores to slow muscle fatigue. Although some of the slowing of fatigue in the diaphragm is due to fiber type changes (increased type I fibers), the ability of higher concentrations of rapamycin to increase the rate of fatigue in the FKBP12-deficient diaphragm suggests that there is also a more direct FKBP12-dependent effect.

It is likely that the transiently increased cytosolic Ca^{2+} concentrations associated with rapamycin/SLF treatments or FKBP12 deficiency contribute to the changes in protein synthesis because Ca^{2+} is required for mTORC1 activation of S6K (39–43). However, the mechanism for this Ca^{2+}-dependent regulation of mTORC1 remains to be elucidated. Rastogi *et al.* (44) found that rapamycin activated both Akt and ERK pathways in macrophages. Another possibility is that the drugs and FKBP12 deficiency increase the activity of Ras at the membrane by promoting its membrane retention and, through the increase in cytosolic Ca^{2+}, activate guanosine nucleotide exchange factor, RasGRP (Ras guanyl-releasing protein 1). RasGRP is regulated by both Ca^{2+} and diacylglycerol (45). Activated Ras could, in turn, activate ERK signaling. The increased ERK signaling by FKBP12 and low dose rapamycin and SLF supports a role for this pathway, and studies are currently under way to determine whether treatment of skeletal muscle fibers with low dose rapamycin or SLF affects Ras localization and phospholipase C activity. Consistent with this pathway, treatment of PC12 cells with FK506 enhances Ras signaling in PC12 cells (46).

In summary (Fig. 10), our findings suggest that beneficial effects of decreased muscle FKBP12 and low dose rapamycin and SLF on adult skeletal muscle function are, at least partially, due to altered regulation of myoplasmic Ca^{2+} handling and increased protein synthesis. Other FKBP12-binding proteins may also contribute to the phenotype. However, we find no evidence of alteration in TGFβ signaling. The current study advances our understanding of skeletal muscle fatigue and regulation of muscle protein synthesis and lays the groundwork for the development of therapeutic interventions for patients with symptoms characterized by enhanced fatigue.

REFERENCES

1. Laplante, M., and Sabatini, D. M. (2012) mTOR signaling in growth control and disease. *Cell* **149,** 274–293
2. Wilkinson, J. E., Burmeister, L., Brooks, S. V., Chan, C. C., Friedline, S., Harrison, D. E., Hejtmancik, J. F., Nadon, N., Strong, R., Wood, L. K., Woodward, M. A., and Miller, R.A. (2012) Rapamycin slows aging in mice. *Aging Cell* **11,** 675–682
3. Spilman, P., Podlutskaya, N., Hart, M.J., Debnath, J., Gorostiza, O., Bredesen, D., Richardson, A., Strong, R., and Galvan V. (2010) Inhibition of mTOR by rapamycin abolishes cognitive deficits and reduces amyloid-β levels in a mouse model of Alzheimer's disease. *PLoS One* **5,** e9979
4. Komarova, E. A., Antoch, M. P., Novototskaya, L. R., Chernova, O. B., Paszkiewicz, G., Leontieva, O. V., Blagosklonny, M. V., and Gudkov, A. V. (2012) Rapamycin extends lifespan and delays tumorigenesis in heterozygous $p53^{+/-}$ mice. *Aging* **4,** 709–714
5. Chan, S. (2004) Targeting the mammalian target of rapamycin (mTOR): a new approach to treating cancer. *Br. J. Cancer* **91,** 1420–1424
6. Ehninger, D., Han, S., Shilyansky, C., Zhou, Y., Li, W., Kwiatkowski, D.J., Ramesh, V., and Silva, A.J. (2008) Reversal of learning deficits in a $Tsc2^{+/-}$ mouse model of tuberous sclerosis. *Nat. Med.* **14,** 843–848
7. Johnson, S. C. (2013) mTOR inhibition alleviates mitochondrial disease in a mouse model of Leigh syndrome. *Science* **342,** 1524–1528
8. Ramos, F. J., Chen, S. C., Garelick, M. G., Dai, D. F., Liao, C. Y., Schreiber, K. H., MacKay, V. L., An, E. H., Strong, R., Ladiges, W. C., Rabinovitch, P. S., Kaeberlein, M., and Kennedy, B. K. (2012) Rapamycin reverses elevated mTORC1 signaling in lamin A/C-deficient mice, rescues cardiac and skeletal muscle function, and extends survival. *Sci. Transl. Med.* **4,** 144ra103
9. Thoreen, C. C., and Sabatini, D. M. (2009) Rapamycin inhibits mTORC1, but not completely. *Autophagy* **5,** 725–726
10. Schreiber, S. L., and Crabtree, G.R. (1995) Immunophilins, ligands, and the control of signal transduction. *Harvey Lect.* **91,** 99–114
11. Avila, G., Lee, E. H., Perez, C. F., Allen, P. D., and Dirksen, R. T. (2003) FKBP12 binding to RyR1 modulates excitation-contraction coupling in mouse skeletal myotubes. *J. Biol. Chem.* **278,** 22600–22608
12. Chen, Y. G., Liu, F., and Massague, J. (1997) Mechanism of TGFβ receptor inhibition by FKBP12. *EMBO J.* **16,** 3866–3876
13. Ahearn, I. M., Tsai, F.D., Court, H., Zhou, M., Jennings, B. C., Ahmed, M., Fehrenbacher, N., Linder, M. E., and Philips, M. R. (2011) FKBP12 binds to acylated H-ras and promotes depalmitoylation. *Mol. Cell* **41,** 173–185
14. Dowling, R. J., Topisirovic, I., Fonseca, B. D., and Sonenberg, N. (2010) Dissecting the role of mTOR: lessons from mTOR inhibitors. *Biochim. Biophys. Acta* **1804,** 433–439
15. Bierer, B. E., Mattila, P. S., Standaert, R. F., Herzenberg, L. A., Burakoff, S. J., Crabtree, G., and Schreiber, S. L. (1990) Two distinct signal transmission pathways in T lymphocytes are inhibited by complexes formed between an immunophilin and either FK506 or rapamycin. *Proc. Natl. Acad. Sci. U.S.A.* **87,** 9231–9235
16. Schiaffino, S., and Reggiani, C. (2011) Fiber types in mammalian skeletal muscles. *Physiol. Rev.* **91,** 1447–1531
17. Yan, Z., Okutsu, M., Akhtar, Y. N., and Lira, V. A. (2011) Regulation of exercise-induced fiber type transformation, mitochondrial biogenesis, and angiogenesis in skeletal muscle. *J. Appl. Physiol.* **110,** 264–274
18. Parsons, S. A., Wilkins, B. J., Bueno, O. F., and Molkentin, J. D. (2003) Altered skeletal muscle phenotypes in calcineurin Aα and Aβ gene-targeted mice. *Mol. Cell Biol.* **23,** 4331–4343
19. Gan, Z., Rumsey, J., Hazen, B. C., Lai, L., Leone, T. C., Vega, R. B., Xie, H., Conley, K. E., Auwerx, J., Smith, S. R., Olson, E. N., Kralli, A., and Kelly, D. P. (2013) Nuclear receptor/microRNA circuitry links muscle fiber type to energy metabolism. *J. Clin. Invest.* **123,** 2564–2575
20. Narkar, V. A., Downes, M., Yu, R. T., Embler, E., Wang, Y. X., Banayo, E., Mihaylova, M. M., Nelson, M. C., Zou, Y., Juguilon, H., Kang, H., Shaw, R. J., and Evans, R. M. (2008) AMPK and PPARδ agonists are exercise mimetics. *Cell* **134,** 405–415
21. Allen, D. G., Kabbara, A. A., and Westerblad, H. (2002) Muscle fatigue: the role of intracellular calcium stores. *Can. J. Appl. Physiol.* **27,** 83–96
22. Braun, P. D., Barglow, K. T., Lin, Y. M., Akompong, T., Briesewitz, R., Ray,

G. T., Haldar, K., and Wandless, T. J. (2003) A bifunctional molecule that displays context-dependent cellular activity. *J. Am. Chem. Soc.* **125,** 7575–7580
23. Tang, W., Ingalls, C. P., Durham, W. J., Snider, J., Reid, M. B., Wu, G., Matzuk, M. M., and Hamilton, S. L. (2004) Altered excitation-contraction coupling with FKBP12 skeletal muscle-specific deficiency. *FASEB J.* **18,** 1597–1599
24. Lanner, J. T., Georgiou, D. K., Dagnino-Acosta, A., Ainbinder, A., Cheng, Q., Joshi, A. D., Chen, Z., Yarotskyy, V., Oakes, J. M., Lee, C. S., Monroe, T. O., Santillan, A., Dong, K., Goodyear, L., Ismailov, I. I., Rodney, G. G., Dirksen, R. T., and Hamilton, S. L. (2012) AICAR prevents heat-induced sudden death in RyR1 mutant mice independent of AMPK activation. *Nat. Med.* **18,** 244–251
25. Shou, W., Aghdasi, B., Armstrong, D. L., Guo, Q., Bao, S., Charng, M.-J., Mathews, L. M., Schneider, M. D., Hamilton, S. L., and Matzuk, M. M. (1998) Cardiac defects and altered ryanodine receptor function in mice lacking FKBP12. *Nature* **391,** 489–492
26. Corona, B. T., Rouviere, C., Hamilton, S. L., and Ingalls, C. P. (2008) FKBP12 deficiency reduces strength deficits after eccentric contraction-induced muscle injury. *J. Appl. Physiol.* **105,** 527–537
27. Bentzinger, C. F., Lin, S., Romanino, K., Castets, P., Guridi, M., Summermatter, S., Handschin, C., Tintignac, L. A., Hall, M. N., and Rüegg, M. A. (2013) Differential response of skeletal muscles to mTORC1 signaling during atrophy and hypertrophy. *Skelet. Muscle* **3,** 6
28. Shioi, T., McMullen, J. R., Tarnavski, O., Converso, K., Sherwood, M.C., Manning, W. J., and Izumo, S. (2003) Rapamycin attenuates load-induced cardiac hypertrophy in mice. *Circulation* **107,** 1664–1670
29. Harrison, D. E., Strong, R., Sharp, Z.D., Nelson, J.F., Astle, C.M., Flurkey, K., Nadon, N.L., Wilkinson, J.E., Frenkel, K., Carter, C.S., Pahor, M., Javors, M.A., Fernandez, E., and Miller, R.A. (2009) Rapamycin fed late in life extends lifespan in genetically heterogeneous mice. *Nature* **460,** 392–395
30. Chaveroux, C., Eichner, L.J., Dufour, C.R., Shatnawi, A., Khoutorsky, A., Bourque, G., Sonenberg, N., and Giguère, V. (2013) Molecular and genetic crosstalks between mTOR and ERRα are key determinants of rapamycin-induced nonalcoholic fatty liver. *Cell Metab.* **17,** 586–598
31. Bellinger, A. M., Reiken, S., Dura, M., Murphy, P. W., Deng, S. X., Landry, D. W., Nieman, D., Lehnart, S. E., Samaru, M., LaCampagne, A., and Marks, A. R. (2008) Remodeling of ryanodine receptor complex causes "leaky" channels: a molecular mechanism for decreased exercise capacity. *Proc. Natl. Acad. Sci. U.S.A.* **105,** 2198–2202
32. Marks, A. R. (1996) Expression and regulation of ryanodine receptor/calcium release channels. *Trends Cardiovasc. Med.* **6,** 130–135
33. Schmidt, E. K., Clavarino, G., Ceppi, M., and Pierre, P. (2009) SUnSET, a nonradioactive method to monitor protein synthesis. *Nat. Methods* **6,** 275–277
34. Rangwala, S. M., Wang, X., Calvo, J. A., Lindsley, L., Zhang, Y., Deyneko, G., Beaulieu, V., Gao, J., Turner, G., and Markovits, J. (2010) Estrogen-related receptor γ is a key regulator of muscle mitochondrial activity and oxidative capacity. *J. Biol. Chem.* **285,** 22619–22629
35. Huss, J. M., Torra, I. P., Staels, B., Giguère, V., and Kelly, D. P. (2004) Estrogen-related receptor α directs peroxisome proliferator-activated receptor α signaling in the transcriptional control of energy metabolism in cardiac and skeletal muscle. *Mol. Cell Biol.* **24,** 9079–9091
36. LaBarge, S., McDonald, M., Smith-Powell, L., Auwerx, J., and Huss, J.M. (2014) Estrogen-related receptor-α (ERRα) deficiency in skeletal muscle impairs regeneration in response to injury. *FASEB J.* **28,** 1082–1097
37. Franzini-Armstrong, C. (1991) Simultaneous maturation of transverse tubules and sarcoplasmic reticulum during muscle differentiation in the mouse. *Dev. Biol.* **146,** 353–363
38. García, J., and Beam, K.G. (1994) Measurement of calcium transients and slow calcium current in myotubes. *J. Gen. Physiol.* **103,** 107–123
39. Mercan, F., Lee, H., Kolli, S., and Bennett, A. M. (2013) Novel role for SHP-2 in nutrient-responsive control of S6 kinase 1 signaling. *Mol. Cell Biol.* **33,** 293–306
40. Graves, L. M., He, Y., Lambert, J., Hunter, D., Li, X., and Earp, H. S. (1997) An intracellular calcium signal activates p70 but not p90 ribosomal S6 kinase in liver epithelial cells. *J. Biol. Chem.* **272,** 1920–1928
41. Hannan, K. M., Thomas, G., and Pearson, R. B. (2003) Activation of S6K1 (p70 ribosomal protein S6 kinase 1) requires an initial calcium-dependent priming event involving formation of a high-molecular-mass signalling complex. *Biochem. J.* **370,** 469–477
42. Gulati, P., Gaspers, L. D., Dann, S. G., Joaquin, M., Nobukuni, T., Natt, F., Kozma, S. C., Thomas, A. P., and Thomas, G. (2008) Amino acids activate mTOR complex 1 via Ca^{2+}/CaM signaling to hVps34. *Cell Metab.* **7,** 456–465
43. Conus, N. M., Hemmings, B. A., and Pearson, R. B. (1998) Differential regulation by calcium reveals distinct signaling requirements for the activation of Akt and p70S6k. *J. Biol. Chem.* **273,** 4776–4782
44. Rastogi, R., Jiang, Z., Ahmad, N., Rosati, R., Liu, Y., Beuret, L., Monks, R., Charron, J., Birnbaum, M. J., and Samavati, L. (2013) Rapamycin induces mitogen-activated protein (MAP) kinase phosphatase-1 (MKP-1) expression through activation of protein kinase B and mitogen-activated protein kinase kinase pathways. *J. Biol. Chem.* **288,** 33966–33977
45. Bos, J. L., Rehmann, H., and Wittinghofer, A. (2007) GEFs and GAPs: critical elements in the control of small G proteins. *Cell* **129,** 865–877
46. Lyons, W. E., George, E. B., Dawson, T. M., Steiner, J. P., and Snyder, S. H. (1994) Immunosuppressant FK506 promotes neurite outgrowth in cultures of PC12 cells and sensory ganglia. *Proc. Natl. Acad. Sci. U.S.A.* **91,** 3191–3195